The Journal of Engineering

The 9th International Conference on Power Electronics, Machines and Drives (PEMD 2018)

IET Journals
The Institution of Engineering and Technology

DC–DC converter with a high step-down ratio for water desalination applications

eISSN 2051-3305
Received on 21st June 2018
Accepted on 27th July 2018
E-First on 15th April 2019
doi: 10.1049/joe.2018.8039
www.ietdl.org

Richard C. Pollock[1] ✉, *Neville McNeill*[1], *Derrick Holliday*[1], *Barry W. Williams*[1]

[1]*Department of Electronic and Electrical Engineering, University of Strathclyde, Glasgow, UK*

✉ *E-mail: richard.pollock@strath.ac.uk*

Abstract: A single-stage 600 : 1 ratio voltage step-down dc–dc converter designed to produce a voltage of between 1 and 1.5 V from a rectified single/three-phase AC supply, for application in a desalination process, is presented. A coupled-inductor design is used, and a novel snubber circuit with energy recovery manages the effects of imperfect coupling (leakage) between the coupled windings. The circuit, which is bidirectional, allows for the power devices to be rated for either high current or high voltage. This presents significant cost and performance advantages compared to a conventional single-stage buck converter where such a large step-down ratio would require a small duty ratio and components with high ratings for both voltage and current: in this case, ratings of 1200 V to withstand input dc voltage switching, and 1000 A to deliver the output current, would be required.

1 Introduction

Capacitive deionisation is a method of water desalination that can offer greater efficiencies than other methods [1]. Two non-touching electrodes are placed in a saline solution, and a voltage is applied across the electrodes causing the ionic bonds in the solution to begin to break. If the voltage across the electrodes is between 1 and 1.5 V, only the sodium chloride ionic bond will break and the hydrogen-oxygen bonds in the water remain intact. The chloride and sodium ions collect at the electrodes until the release or flushing phase, which creates a voltage across the electrodes by allowing the ions to recombine in the water. As such, the energy used in the process is minimal due to the recovery of energy by flushing the electrodes into brackish water. This method requires a mains-powered bidirectional circuit that can produce a voltage below 1.5 V and a current of the order 250–1000 A. A coupled-inductor design [2, 3] is investigated in this paper.

In the proposed circuit shown in Fig. 1, Q_1 is the main switch, and Q_2 is switched in anti-phase as a synchronous rectifier. The coupled inductor L_1 has a turns ratio $N_1 : N_2$ of 100 : 1.

2 Circuit operation

2.1 Mode 1

When Q_1 is turned on (Fig. 2), a dc voltage of 340–600 V (corresponding to rectified single- or three-phase AC, respectively) is applied across the coupled inductor L_1. Current flows through output load resistance R_1, via both windings N_1 and N_2 of the coupled inductor and through Q_1 to 0 V (solid, red). Some of the energy from the input is used to charge C_1 (dotted, blue). Whilst the main switch Q_1 is on, Q_3 is also on as both are controlled by the same gating signal. Snubber capacitor C_2 discharges through transformer T1 (dashed, orange) during 'on' period of switches Q_1 and Q_3. This induces a positive voltage on the secondary of T1 and creates a current through D5 (sparse dotted, green).

2.2 Mode 2

When Q_1 is turned off, current freewheels through the secondary winding N_2 of the coupled inductor L_1 and through synchronous rectifier Q_2, and supplies load resistance R_1 (solid, red). When Q_1 is off, the peak current in N_2 is 100 times the amplitude of the on-time current through Q_1. Output capacitor C_1 is referenced to the positive supply rail and delivers a low-voltage output to the desalination electrodes (dotted, blue) represented by load resistance R_1. The main switch Q_1 does not carry the high output current and the synchronous rectifier Q_2 only needs a low voltage rating. Thus, a low $R_{DS(on)}$ device can be selected and power loss minimised during high current flow. The topology can be rearranged so that the load is referenced to 0 V.

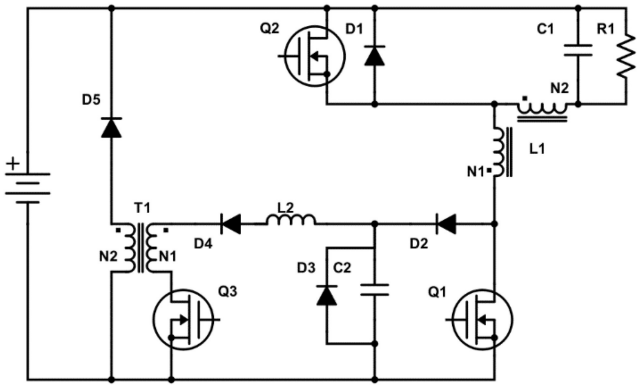

Fig. 1 *Coupled inductor buck converter with regenerative fly-forward snubber*

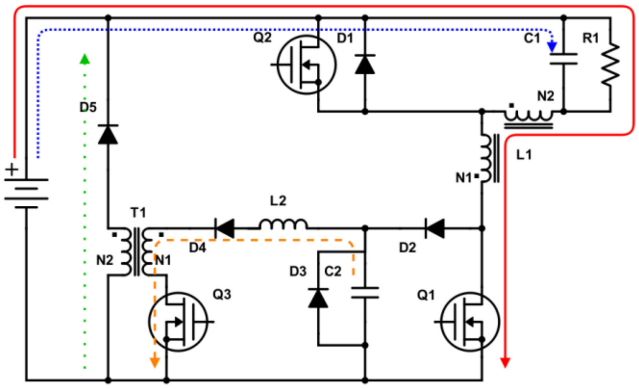

Fig. 2 *Mode 1 – energising coupled inductor L_1*

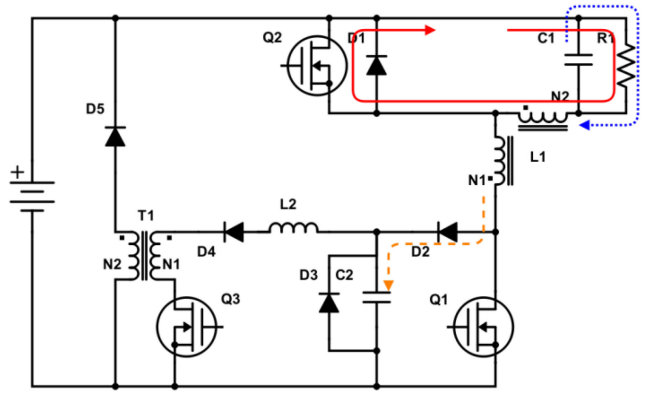

Fig. 3 *Mode 2 – Q_1 turned off*

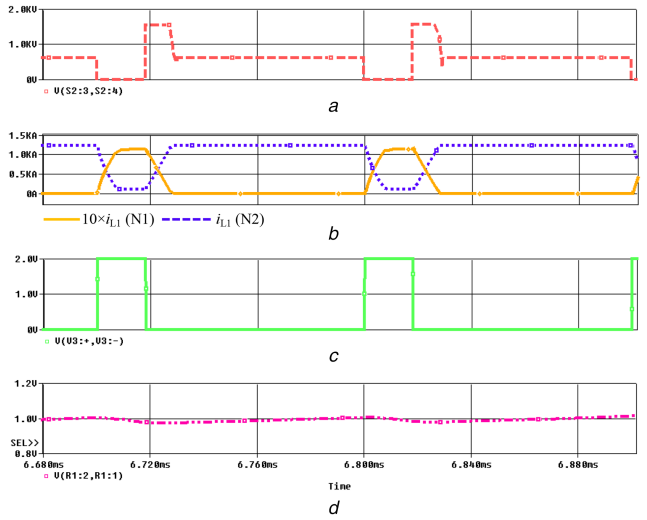

Fig. 4 *Circuit waveforms*
(a) Voltage across Q_1, ***(b)*** L_1 inductor current, ***(c)*** Q_1 gate signal, ***(d)*** output voltage across R_1

In Mode 2 the current in the N_1 winding of L_1 falls to zero. Magnetic flux in L_1 is maintained by current flowing through N_2 where, due to the turns ratio, the amplitude of this current is 100 times greater than that flowing prior to Q_1 switching off. This current freewheels through synchronous rectifier Q_2 and load R_1. Snubber capacitor C_2 absorbs excess current (dashed, orange) caused by the leakage inductance of coupled inductor L_1, ensuring no overvoltage on Q_1.

2.3 Snubber operation

When Q_1 switches off, turn-off snubber capacitor C_2 recovers the significant leakage energy of the coupled inductor L_1 [4]. Q_1 and Q_3 utilise the same drive signal, resulting in a simple control structure. When both Q_1 and Q_3 are turned on, the turn-off snubber is reset. C_2 resonates current through L_2 into forward coupled transformer T1, so that the snubber energy is returned to the input supply. The energy recovery circuit is adaptive: when load current increases, snubber action occurs at a lower voltage level, giving better switch protection whilst recovering snubber energy. This adaptation is achieved by fixing the turns ratio of T1 so that the reflected resonant circuit voltage is greater than half the dc-link voltage. Under light load, the snubber capacitor does not fully discharge. As the load current increases there is more leakage energy in coupled inductor L_1, the bypass diode D3 conducts, clamping the snubber capacitor voltage to zero, thereby allowing the voltage transients to be supressed (Fig. 3).

3 Simulation

Table 1 Primary components of the dc–dc converter

Name	Component	Model	Rating
Q_1	MOS power transistor	IPB100N	30 V
Q_2	power MOSFET	IGW15N$_1$20H3	1700 V
D2-5	diode D2PAK	ISL$_9$R$_1$8120S3ST	1700 V
C_1	electrolytic capacitor	ELH689M016AT6AA	68,000 µF

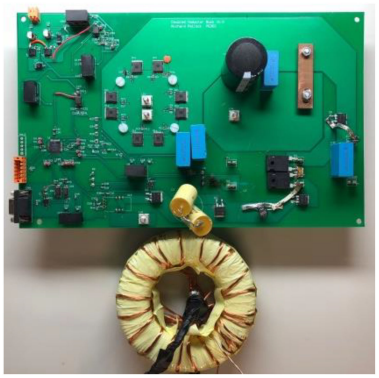

Fig. 5 *Coupled inductor circuit prototype*

Fig. 4 shows simulation results for output current of 1000 A at 1 V, derived from a $600V_{dc}$ supply. In Fig. 4*a*, the voltage across the main switch Q_1 is limited to a peak value of ~1.4 kV by the fly-forward snubber, allowing a 1.7 kV rated device to be used. The snubber capacitor (C_2) voltage is reset by Q_3, and energy is recovered back into the dc supply. Fig. 4*b* shows the interchange of current in the primary (N_1) and secondary (N_2) windings of coupled inductor L_1, with the turns ratio of 10 : 1 delivering 1000 A to the load with only 100 A in Q_1, i.e. the current in N_1 is ten times smaller than that N_2 as a result of the 10 : 1 turns ratio. The coupling factor used in the simulations was 0.98. This can be seen from the time it takes the energy to couple from N_1 to N_2 in Fig. 4*b*. The duty ratio of Q_1 is approximately 20%, as shown in Fig. 4*c*. Fig. 4*d* shows the output voltage.

4 Experimentation

The experimental system consists of the proposed dc–dc converter and a microcontroller. Communication lines and the microcontroller are controlled area network controlled. The microcontroller samples current and voltage measurements at 40 kHz, and records real-time temperature measurements for protection of the devices. The printed circuit board was designed to minimise resistance of current paths and to ensure balanced signal impedances. Switch Q_2, used as a synchronous rectifier, comprises eight parallel-connected MOSFETs, switched at the same time to ensure equal current sharing. The main components used in the dc–dc converter are summarised in Table 1, and the circuit is shown in Fig. 5. Simulation showed that poor inductor coupling causes switching voltages that can exceed device ratings. To minimise leakage inductance [4], therefore, coupled inductor L_1 was densely wound to ensure maximum coupling. An iron powder T520-52 core was used. The N_1 winding consisted of 125 turns of copper wire. The N_2 winding was formed from 12 parallel-connected coils, each having two turns. The resulting $N_1 : N_2$ turns ratio was 62 : 1. This was not the targeted ratio (100 : 1) but was the maximum that could be achieved with the core whilst maintaining minimal leakage inductance.

4.1 Coupled inductor calculations

4.1.1 RMS current: Ampere-turn balance dictates that the magnetomotive forces in the main coupled inductor L_1 must be equal before and after each transition between Mode 1 (on state)

and Mode 2 (off state). The current I_1 in N_1 and the current I_2 in N_2 are therefore related by

$$I_2(\text{off})N_2 + I_1(\text{off})N_1 = I_2(\text{on})N_2 + I_1(\text{on})N_1 \quad (1)$$

Since $I_1(\text{off}) = 0$ and $I_2(\text{on}) = I_1(\text{on})$

$$I_2(\text{off})N_2 = I_2(\text{on})N_2 + I_2(\text{on})N_1 \quad (2)$$

Rearranging (2) gives

$$\frac{I_2(\text{off})}{I_2(\text{on})} = \frac{N_1 + N_2}{N_2} \quad (3)$$

The average current in N_2 is

$$I_{\text{ave}} = \delta I_2(\text{on}) + (1 - \delta)I_2(\text{off}) \quad (4)$$

Substituting for $I_2(\text{off})$ gives

$$I_{\text{ave}} = \delta I_2(\text{on}) + (1 - \delta)I_2(\text{on})\frac{N_1 + N_2}{N_2} \quad (5)$$

Rearranging (5) gives

$$I_2(\text{on}) = \frac{I_{\text{ave}}}{\delta + (1 - \delta)((N_1 + N_2)/N_2)} \quad (6)$$

$I_2(\text{off})$ is then calculated as

$$\begin{aligned} I_2(\text{off}) &= \frac{I_{\text{ave}}}{\delta + (1 - \delta)((N_1 + N_2)/N_2)} \times \frac{N_1 + N_2}{N_2} \\ &= \frac{I_{\text{ave}}}{\delta((N_1 + N_2)/N_2) + (1 - \delta)} \end{aligned} \quad (7)$$

Rearranging (7) to give I_{ave} and taking the square root to calculate $I_2(\text{RMS})$ gives

$$I_2(\text{RMS}) = \sqrt{\delta I_2(\text{on})^2 + (1 - \delta)I_2(\text{off})^2} \quad (8)$$

This is the relationship between RMS current and duty cycle. The RMS current in conjunction with the number of turns required determines the wire gauge required to realise coupled inductor L_1.

4.1.2 Number of turns: In any given inductor L with N turns, the flux $\varnothing$ and current I are related by

$$L\frac{\text{d}i}{\text{d}t} = N\frac{\text{d}\varnothing}{\text{d}t} \rightarrow L\text{d}i = N\text{d}\varnothing \quad (9)$$

Integrating (9) to obtain inductance L gives

$$L = \frac{NAB}{i} \quad (10)$$

Expressing B in terms of the physical properties of the core gives

$$L = \frac{NA\mu_o\mu_r Ni}{li} = \frac{A\mu_o\mu_r N^2}{l} \quad (11)$$

Rearranging (11) in terms of N gives

$$N = \sqrt{\frac{L \times l}{A \times \mu_0 \times \mu_r}} \quad (12)$$

where l is the magnetic path length and A is the cross-sectional area of the core

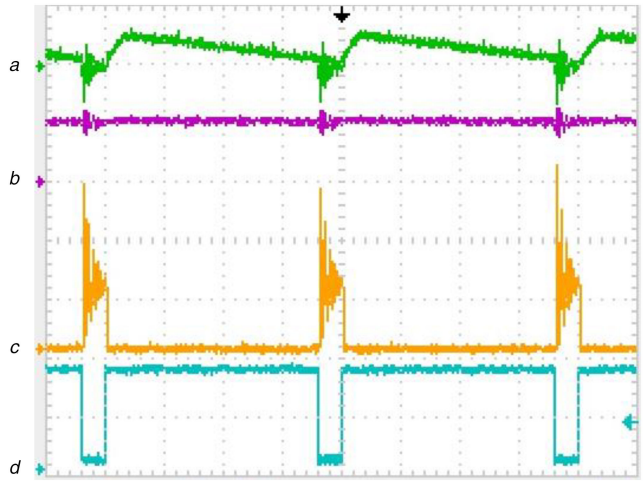

Fig. 6 *Discontinuous operation with reverse current flow (timebase 25 µs/div)*
(a) current through L_1 (N_2) (5 A/div), ***(b)*** output voltage (1 V/div), ***(c)*** voltage across Q_2 (10 V/div), ***(d)*** Q_2 gate signal (2 V/div)

$$N = \sqrt{\frac{5 \times 10^{-3} \times 310.9 \times 10^{-3}}{796.1 \times 10^{-6} \times 1.2566 \times 10^{-6} \times 100}} = 124.7 \text{ turns} \quad (13)$$

If a turns ratio of 1 : 100 is used, based on (13) $N_2 = 1.24$ turns which is impractical. Peak saturation current occurs at the beginning of Mode 2 when only N_2 carries current. This can be calculated from (14) to (16)

$$\text{saturation flux density } B_s = \frac{I_{\text{peak}} \times N}{l} \quad (14)$$

$$I_{\text{peak}} = \frac{B_s \times l}{N} \quad (15)$$

Inserting design values gives

$$I_{\text{peak}} = \frac{500 \times 310.9 \times 10^{-3}}{1.24} = 125 \text{ A} \quad (16)$$

4.2 Proof of concept

The dc–dc converter was initially operated at low power with a coupled inductor L_1 turns ratio $N_1 : N_2$ of 1 : 16. This showed that the design was working as intended. However, some issues were noted.

At start-up, if not controlled, current can flow through the synchronous switch Q_2 in the reverse direction. Until continuous steady-state operation is reached, therefore, the synchronous switch is held in the off state. If the current in the secondary inductor N_2 drops to 0 A, highlighted by the discontinuous operation shown in Fig. 6, current can flow in the reverse direction via the synchronous switch Q_2 to the output. When Q_1 turns back on, the voltage across Q_2 rises rapidly due to the flux in the core of L_1 having to be reversed before current can flow through Q_1. This would not usually be an issue as the voltage spike is only around 30 V. Due to the desire to use a very low $R_{\text{DS(on)}}$ device, however, a 30 V spike would be detrimental to the circuit.

Once continuous inductor current operation is reached, as shown in Fig. 7, the main switch Q_1 turns on and current in the N_1 rises rapidly. This is due to existing current flowing in N_2 coupling back into the N_1. The point at which the currents in N_1 and N_2 become equal is highlighted in Fig. 7 by a change in current gradient. At this point, N_1 and N_2 effectively become series connected. The main switch Q_1 is then turned off and the energy couples back into N_2.

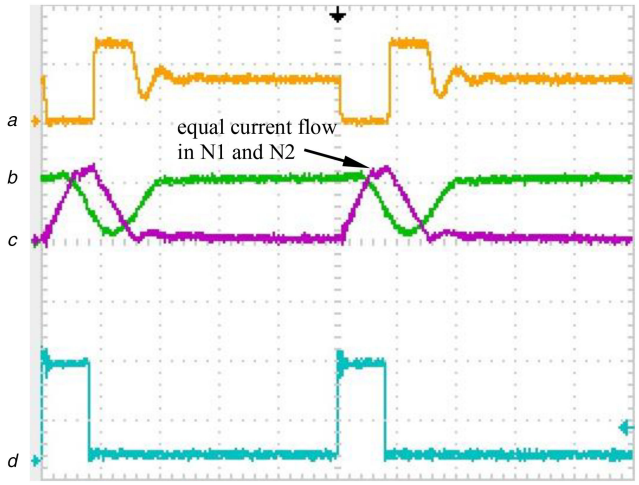

Fig. 7 *Continuous operation and coupled inductor current transferring from N_1 to N_2 (timebase 5 µs/div)*

(a) Voltage across Q_1 (N_2) (100 V/div), ***(b)*** L_1 (N_2) current (2 A/div), ***(c)*** L_1 (N_1) current (0.5 A/div), ***(d)*** Q_1 gate signal (2 V/div)

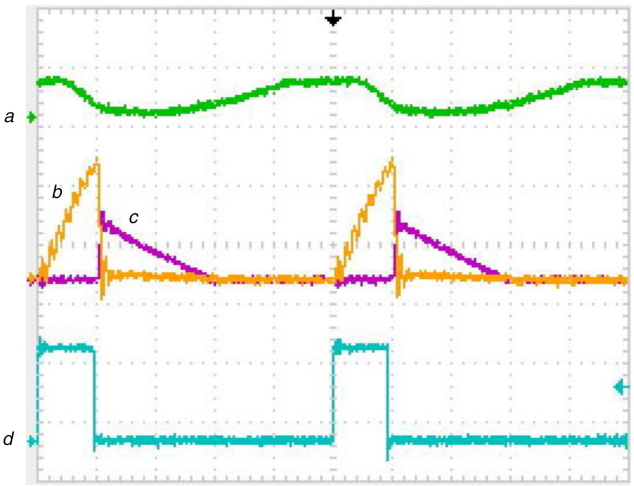

Fig. 9 *Flyback snubber with $N_1 : N_2 = 2 : 1$ turns ratio (timebase 5 µs/div)*

(a) L_1 (N_2) current (5 A/div), ***(b)*** T1 primary current (1 A/div), ***(c)*** T1 secondary current (1 A/div), ***(d)*** Q_1 gate signal (2 V/div)

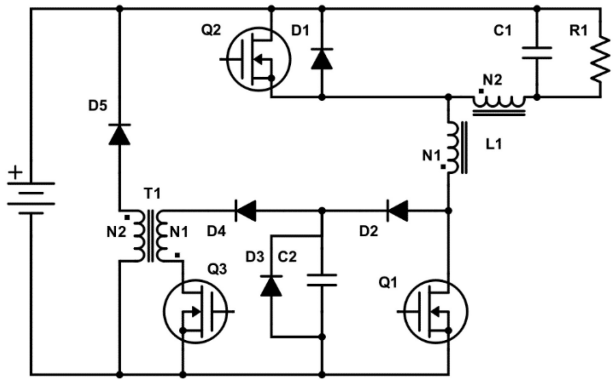

Fig. 8 *Snubber circuit modified to a flyback configuration*

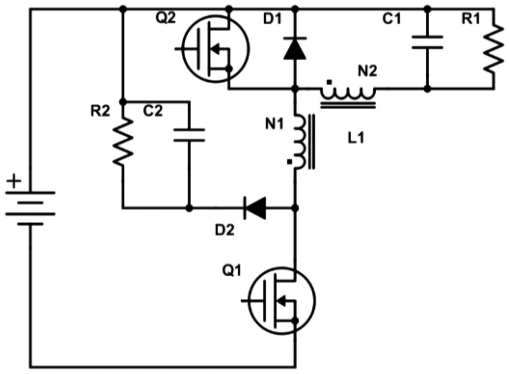

Fig. 10 *Passive snubber implementation*

4.3 Snubber development

Fig. 7*a* shows the voltage across Q_1, which drops to zero when Q_1 is turned on and rises to the snubber voltage at turn off, preventing an overvoltage. The snubber capacitor is discharged by Q_3 when it and Q_1 are switched on. The voltage across Q_3 at turn off may be large due to the absence of a freewheel path for the energy recovery inductor. A flyback snubber, as shown in Fig. 8, was found to be more effective at discharging the snubber capacitor C_2. The current which is built up in N_1 of T1 is transferred to the N_2 of T1 when Q_3 is switched off, as shown in Fig. 9. The current in N_2 is stepped down due to the 2 : 1 turns ratio of T1.

However, limited energy is coupled from the primary N_1 into the secondary N_2 in the main coupled inductor circuit. This is due to the regenerative snubber preventing the voltage across Q_1 rising above the rail voltage. For energy transfer from the primary to the secondary winding, a voltage difference is required. The voltage across Q_1 must be above the input voltage, and the greater this difference the faster the energy transfer. Due to the snubber only allowing a voltage slightly above the input voltage, the energy takes too long to transfer from the primary into the secondary, so is not able to transfer within the oscillatory period.

An ideal snubber would provide infinite resistance until a set voltage is reached and then provide voltage clamping to ensure no further voltage increase. The set voltage should be as high as possible while not risking an overvoltage across the switch. For a 1.7 kV device, a total snubber voltage of 1.5 kV would be acceptable. This can be achieved either passively [3], or using a switch mode power supply (SMPS). The passive circuit, shown in Fig. 10 comprises diode D2 in series with parallel connected resistor R_2 and capacitor C_2. The resistor allows the voltage across switch Q_1 to exceed 600 V, ensuring the diode is not forward biased at too low a voltage.

Fig. 11 illustrates the operation of the passive snubber [5] shown in Fig. 10. Figs. 11*a* and *b* show the currents in the coupled inductor L_1 windings N_1 and N_2, respectively. Fig. 11*c* shows that the voltage across Q_1, is limited to twice the input voltage (288 V in this case, due to power supply availability). The SMPS solution shown in Fig. 12 uses a snubber capacitor C_2 connected between the input and the diode D2. The capacitor voltage is maintained at 1.5 kV by the controlled step up/down SMPS circuit. If only steady-state operation is required, the step up/down SMPS converter can operate with a constant duty cycle. The snubber would be inactive until diode D2 becomes forward biased. Controlling the voltage across C_2 limits the voltage across Q_1. The SMPS snubber gives the same results as the passive RC variant but is more efficient as energy is recovered back into the supply. Diode D4 may be required to prevent a return path for the capacitor current due to the resonant LC circuit.

Simulation results demonstrating the feasibility of the SMPS snubber approach are shown in Fig. 13.

5 Conclusions

A bidirectional single-stage converter circuit for a desalination process, with a voltage step-down ratio of 600 : 1, uses of a coupled inductor within a buck dc–dc converter. Management of the coupled inductor leakage energy was investigated and several snubber circuits were assessed. Two snubber designs are proposed: a simple cheap and effective passive solution, and an efficient energy recovery snubber that requires control. The proposed converter is cost-effective and advantageous when compared to a conventional single-stage buck converter. Achieving a large step-

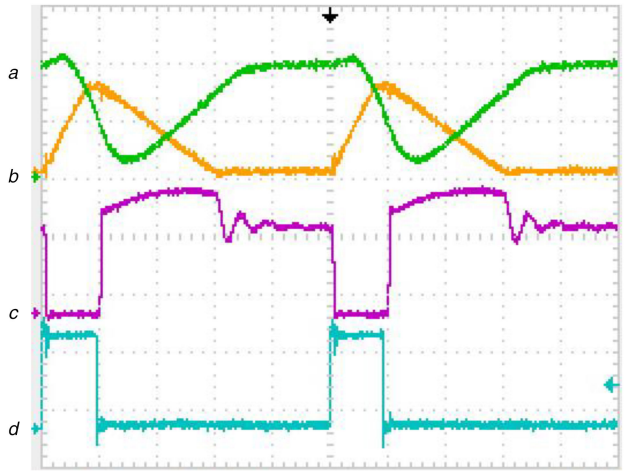

Fig. 11 *Passive RC snubber (timebase 5 µs/div)*
(a) L_1 (N_2) current (50 A/div), ***(b)*** L_1 (N_1) current (2 A/div), ***(c)*** voltage across Q_1 (200 V/div), ***(d)*** Q_1 gate signal (2 V/div)

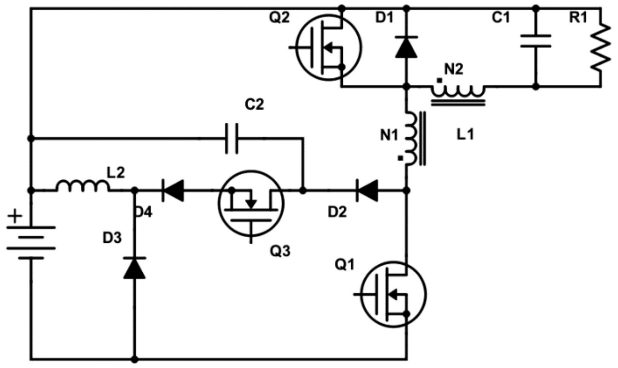

Fig. 12 *SMPS regenerative snubber, using a step-down topology*

down ratio in a single switching stage increases circuit efficiency meaning a significant reduction in the energy required for water desalination.

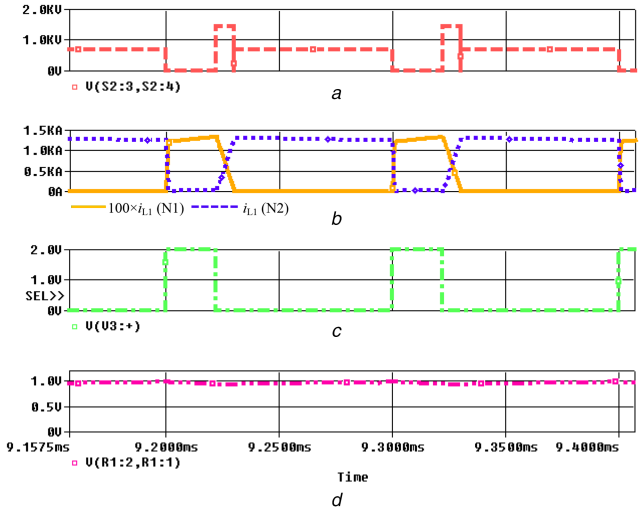

Fig. 13 *Simulation results for the SMPS regenerative snubber showing a current ratio of 1100 is feasible*
(a) Voltage across Q_1, ***(b)*** L_1 inductor current, ***(c)*** Q_1 gate signal, ***(d)*** output voltage across R_1

6 References

[1] Anderson, M.A., Cudero, A.L., Palma, J.: 'Capacitive deionization as an electrochemical means of saving energy and delivering clean water. Comparison to present desalination practices: will it compete?', *Electrochim. Acta*, 2010, **55**, (12), pp. 3845–3856

[2] Williams, B.W.: 'Unified synthesis of tapped-inductor DC-to-DC converters', *IEEE Trans. Power Electron.*, 2014, **29**, (10), pp. 5370–5383

[3] Yao, K., Ye, M., Xu, M., *et al.*: 'Tapped-inductor buck converter for high-step-down DC–DC conversion', *IEEE Trans. Power Electron.*, 2005, **20**, (4), pp. 775–780

[4] Modeer, T., Zdanowski, M., Nee, H.-P.: 'Design and evaluation of tapped inductors for high-voltage auxiliary power supplies for modular multilevel converters'. 15th Int. Power Electronics and Motion Control Conf. and Exposition, EPE-PEMC 2012 ECCE Europe, Novi Sad, Serbia, 2012

[5] Finney, S.J., Williams, B.W., Green, T.C.: 'RCD snubber revisited', *IEEE Trans. Ind. Appl.*, 1996, **32**, (1), pp. 155–160